Sensing via optical interference

by Ryan C. Bailey*, Mohammed Parpia, and Joseph T. Hupp

Chemical and biological sensing are problems of tremendous contemporary technological importance in multiple regulatory and human health contexts, including environmental monitoring, water quality assurance, workplace air quality assessment, food quality control, many aspects of biodiagnostics, and, of course, homeland security. Frequently, what is needed, or at least wanted, are sensors that are simultaneously cheap, fast, reliable, selective, sensitive, robust, and easy to use. Unfortunately, these are often conflicting requirements. Over the past few years, however, a number of promising ideas based on optical interference effects have emerged. Each is based to some extent on advances in the design and fabrication of functional materials. Generally, the advances are of two kinds: chemo- and bio-selective recognition and binding, and efficient methods for micropatterning or microstructuring.

Department of Chemistry,
Northwestern University,
Evanston, IL 60208, USA
E-mail: rbailey@caltech.edu
and j-hupp@northwestern.edu

*Current address:
Division of Chemistry,
California Institute of Technology,
Pasadena, CA 91125, USA

The ability to micropattern materials, especially hard electronic materials like Si, has, of course, existed for some time. More recently, soft lithography techniques like microcontact printing and micromolding have made it easy to micropattern materials such as synthetic or biological polymers[1]. Colloidal crystallization and subsequent infiltration is an interesting way of making periodically microstructured composite materials[2,3]. Yet another is electrochemical or photoelectrochemical oxidation. This approach can be used to make both porous alumina[4] and porous Si[5] (PS) with good spatial control. What makes materials patterning of this kind so interesting for optical sensors is that the length scales are right for engendering optical interference effects in the visible region of the electromagnetic spectrum. The essence of sensing in this way is the modulation of interference behavior by analyte binding.

Interference-based sensing

When light passes through a material, it interacts with the material's electrons and is slowed by a factor of *n* called the refractive index. The magnitude of *n* depends on the polarizability of the material. It can range, for example, from ~1 for air (essentially vacuum) to 1.33 for water, 1.4-1.5 for biopolymers, 2.4 for TiO_2, and 3.8 for Si. Consider the case of light passing from air into a thin film (say, a fraction of the wavelength of the light in thickness) coating a reflective

ISSN:1369 7021 © Elsevier Ltd 2005

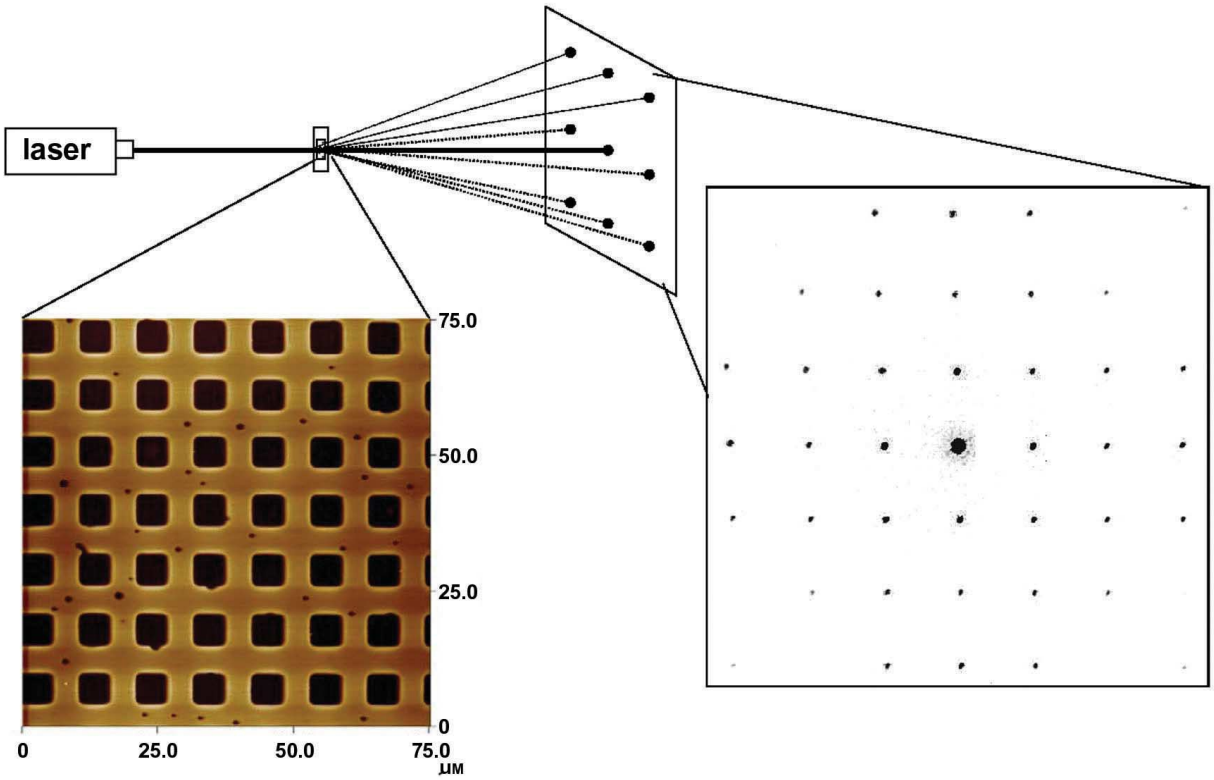

Fig. 1 (top) Diagram of the diffraction of monochromatic light by a grating. (left) A glass-supported diffraction grating fabricated from a polymeric material. (right) The resulting diffraction pattern. The center spot is undiffracted light.

surface. Depending on how far and how quickly they move, light waves exiting the film after reflection can reinforce or cancel those entering it. The relationship between wavelength (λ) and film thickness (d) that maximizes constructive interference is:

$$\lambda_{max} = 2nd/m \quad (1)$$

where m is the spectral order. For a comparatively thick film ($2nd >> \lambda_{visible}$), many wavelengths in the visible region satisfy eq 1 and a plot of reflected light intensity versus wavelength is periodic.

Another structure that generates interference is a grating: a periodic structure consisting of alternating regions of high and low refractive index (see Fig. 1). Monochromatic light that has been transmitted or reflected by a grating forms a spatial pattern of bright spots (diffracted light) that is related to the physical pattern of the grating by an optical transform. The locations of the spots are fixed by the lateral spacing of the grating elements and by the wavelength of the incident light. The efficiency of the grating (the fraction of incident light diffracted) depends on the product of the grating depth and the degree of refractive index contrast between high- and low-index regions of the grating, $d \cdot \Delta n$.

All of the sensors described below make use of optical diffraction, thin-film interferometric reflection, or closely related ideas. The interaction of a micropatterned, microstructured, or micro/mesoporous material with an analyte changes n, Δn, or lattice dimensions in a way that increases or decreases the amount of light reaching a detector, allowing for its detection and quantification.

Fabry-Pérot-like sensors

Illumination of transparent thin-film coatings on reflective surfaces produces so-called Fabry-Pérot fringes – alternating high- and low-intensity features – in the resulting reflection spectrum (see Fig. 2). The spectral peaks appear, as noted above, at $\lambda_{max} = 2nd/m$, where n is the volume-averaged refractive index of the film. Sailor and coworkers[6-18] point out that, if a porous film is used, n will increase when the initially empty pores are filled with analyte. They illustrate the idea using PS films on highly reflective nonporous Si platforms, and describe several examples of volatile organic

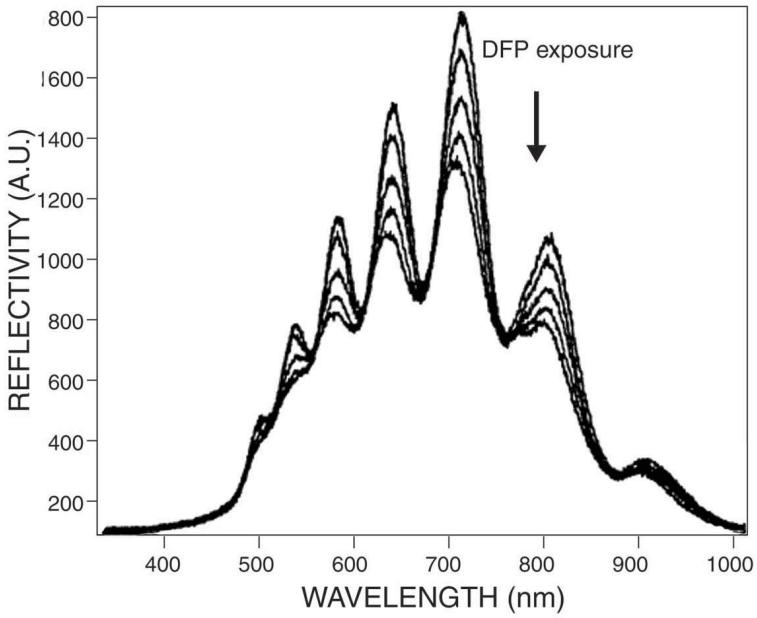

Fig. 2 The reflectivity of a PS film illustrating Fabry-Pérot-like interference fringes. The sharpness of the fringes decreases over time because of etching by HF, a product of the catalytic hydrolysis of a nerve-agent simulant. The response can be used as a means for sensing the agent. (Reprinted with permission from[12]. © 2000 American Chemical Society.)

chemical detection. While these signals are largely because of capillary condensation of volatile organics within the small PS pores, some degree of chemical selectivity can be engendered by grafting appropriate functional groups onto the PS surfaces – the most interesting case perhaps being the detection of CO_2 with amine-derivatized PS[17].

Aqueous-phase sensing of biological macromolecules has also been demonstrated. These have higher indices than the water they displace from the film pores, so the volume-averaged value of *n* increases and the Fabry-Pérot fringes red-shift. Rothberg and coworkers[19] have shown how one-dimensional porous films of electrochemically etched alumina can be used in this way. They illustrate the idea by detecting single-stranded DNA using films derivatized with complementary strands. They point out that porous alumina could offer advantages relative to PS in applications where pore size uniformity is important.

An interesting application that achieves transduction in a different way is one involving the sensing of organofluorophosphonates (chemical warfare agents or simulants)[12]. A Cu-based hydrolysis catalyst is incorporated into the PS assembly and used to degrade the simulant rapidly. One of the hydrolysis products is hydrofluoric acid, which dissolves the SiO_2 present as a thin native coating on the high-area PS surface. The dissolution is observed spectrally as both a blue-shift of the interference fringes and a decrease in definition of the fringes (Fig. 2). Recently, an elegant extension of the general idea of interferometric thin-film sensing has resulted in self-orienting, remotely addressable interferometric sensing particles, termed 'smart dust' (Fig. 3)[16,18].

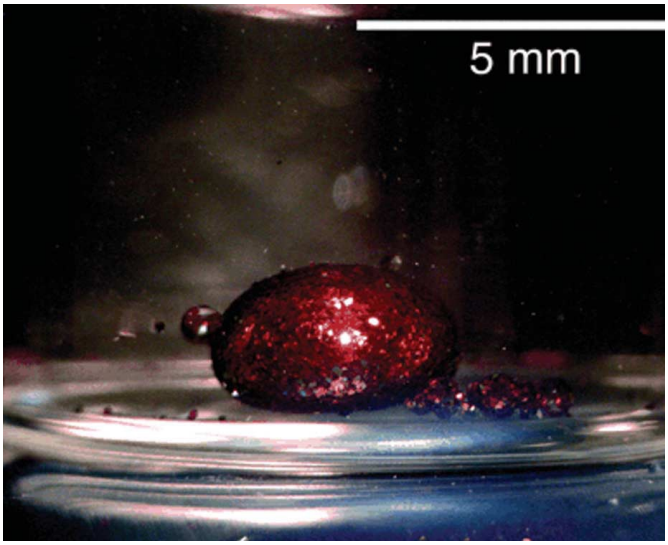

Fig. 3 Optical photograph of the bifunctional PS smart-dust particles assembled at the interface of a small drop of dichloromethane in a vial of water. The particles contain a hydrophobic green mirror and a hydrophilic red mirror on opposite sides. The red mirror is presented to the viewer. (Reprinted with permission from[18]. © 2003 National Academy of Sciences, USA.)

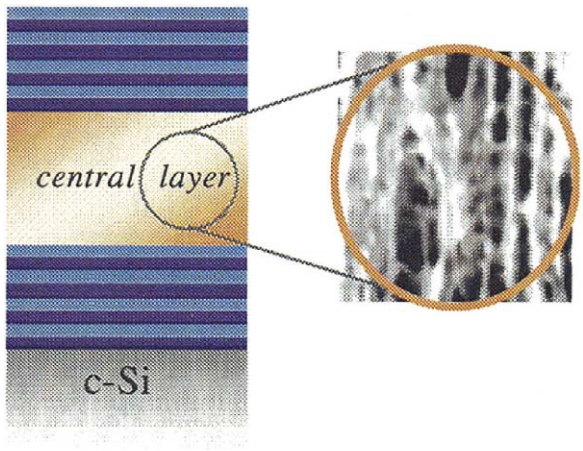

Fig. 4 Structure of a PS microcavity resonator. A central active layer of PS is flanked by a PS multilayer mirror. (Reprinted with permission from[20]. © 2001 American Chemical Society.)

Luminescent interferometric sensors

PS materials often exhibit a broad photoluminescence in the red part of the visible spectrum. Miller and coworkers[20] point out that, with the right kind of microstructure, interferences can be set up and the broad emission envelope can be replaced with one showing evenly spaced spikes, each only a few nanometers wide. The structure is a relatively thick luminescent layer (a few microns thick) sandwiched between a pair of distributed Bragg reflectors (DBRs), as shown in Fig. 4. The structure, while elaborate, is relatively straightforward to construct electrochemically, provided that careful attention is paid to etching times and conditions.

Collectively, the mirrors and active layer comprise a resonator that allows emitted light to escape the cavity only at certain well-defined wavelengths, determined both by the thicknesses and refractive indices of the DBR layers. Filling the pores in a layer with analyte changes the layer's average refractive index, with the change being greater for a high-porosity layer than a low-porosity layer. Sensing is accomplished by monitoring the shift in wavelength of a photoluminescence peak (Fig. 5). Of course, for a narrower peak, the shifts are discerned more easily and the analytical sensitivity of the resonator is increased.

Colloidal crystals

An interesting family of sensors has been developed by Asher and coworkers[21-31] based on the idea of photonic crystals. The crystals are Bragg lattices and transmit light at most wavelengths, but reflect it (via diffraction) over a narrow

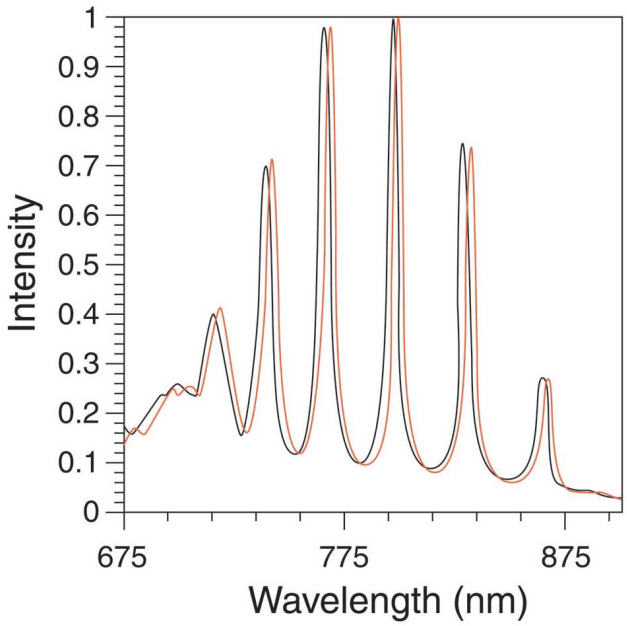

Fig. 5 Photoluminescence from a PS microcavity derivatized with receptors for gram-negative bacteria. The observed peak shifts are in response to bacteria exposure and binding. In the absence of the microcavity structure, only a broad, featureless emission spectrum is seen. (Reprinted with permission from[20]. © 2001 American Chemical Society.)

spectral range centered at λ_{max} from the Bragg equation. Useful crystals can be made from colloidal suspensions of uniformly sized polymeric spheres. When sphere diameters lie between ~100-300 nm, λ_{max} falls in the visible region. Asher and coworkers showed a number of years ago how this behavior could be used to create narrow spectral filters[32].

To make lattices that work as sensors, polymeric polystyrene spheres are assembled into three-dimensional colloidal crystals, and are chemically crosslinked with a hydrogel. The polystyrene component of these unusual mesostructured materials provides the periodicity needed for diffraction while the hydrogel imparts the chemical sensitivity (see Fig. 6). Upon exposure to the right analyte, the hydrogel swells, changing the average refractive index of the lattice and altering λ_{max}. Much more important, though, is the effect of swelling on the interplane spacing or lattice constant, *d*. A 0.5% change in gel volume typically translates into a ~1 nm shift in λ_{max}. Swelling can increase sphere-packing distances by as much as 60% and shift λ_{max} from the blue end of the visible spectrum to the red end (Fig. 7). The effect is striking visually: structured assemblies of colorless components change color in response to colorless analytes!

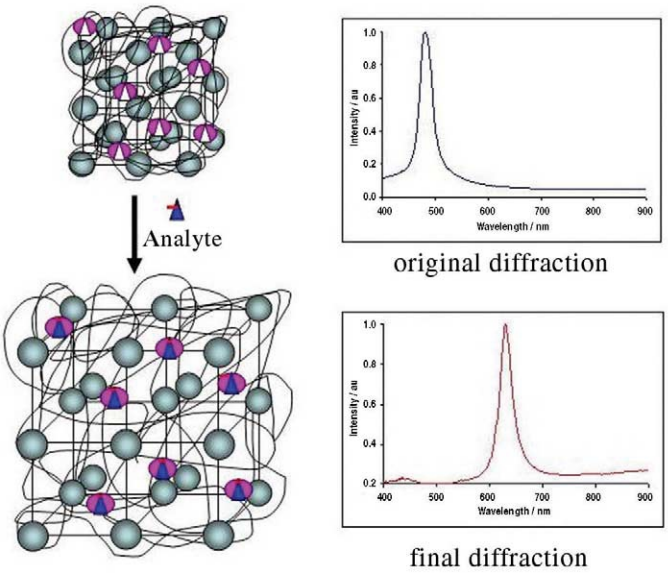

Fig. 6 Schematic of colloidal crystal swelling and lattice expansion in response to analyte binding. (Courtesy of Sandy Asher, University of Pittsburgh.)

Swelling in the derivatized polyacrylamide gels used in this approach is mainly an osmotic pressure effect. For example, partially hydrolyzed gels contain pendant carboxylic acid groups. Upon contact with a high-pH solution, the groups are deprotonated. Charge-compensating cations enter the gel, creating an osmotic pressure sufficient to swell the gel with solvent. At least in the vicinity of the carboxylic acid pK_a, the material becomes an optical reporter on sample solution pH[23].

By functionalizing neutral gels with crown ethers that selectively bind Pb^{2+}, the same principle can be used to make a reflection-based 'optrode'[29] specific for Pb^{2+}. Related schemes can be used to make colloidal crystalline array sensors for neutral molecules, with one of the most interesting applications being a sensor for glucose. Hydrogels derivatized with both boronic acid and poly(ethyleneglycol) bind glucose selectively over other sugars at physiologically relevant concentrations. Once bound, the glucose slightly alters the boronic acid pK_a, triggering gel swelling and engendering an apparent color change in a colloidal crystal array[26]. Because hydrogels tend to be biocompatible, this opens up the exciting possibility of a simple and rapid patient-wearable, patient-monitorable sensor for use by diabetics. A color-changing glucose sensor of millimeter size could be incorporated, for example, in a contact lens and positioned for high contrast over a white portion of the eye[30].

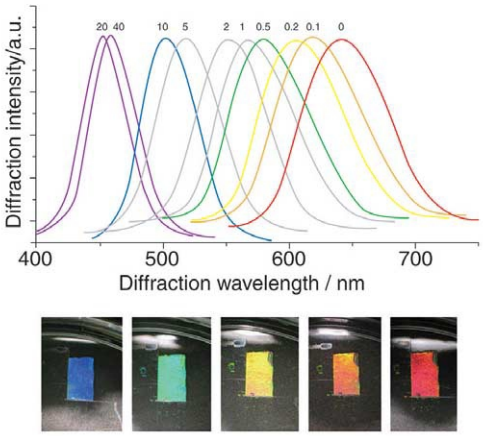

Fig. 7 (top) Diffraction (reflection) intensity spectra for a colloidal crystal experiencing varying degrees of analyte (glucose)-induced swelling. (bottom) Reflection-based color changes (red to blue) of a colloidal crystal upon exposure to glucose solutions of varying concentration. (Courtesy of Sandy Asher, University of Pittsburgh.)

Holographic biosensors

Taking advantage of the same physics underlying colloidal crystals, a family of biosensors has been developed by Lowe and coworkers based on holographic polymer films[33-35]. Upon exposure to a laser beam, reflective holograms are recorded as silver holographic fringes within a polymeric thin film. Analogous to standard interference filters, these films display wavelength-dependent optical properties, with the spectral response dictated by fringe spacing. When holograms are constructed from chemically responsive polymers, the wavelength of maximum reflection λ_{max} is modulated by analyte-induced volume changes.

By monitoring changes in λ_{max}, holograms sensitive to a wide range of analytes have been demonstrated with selectivities determined by the chemical properties of the polymer(s) comprising the holographic medium. While these reports use a spectrophotometer to detect a target species, an intriguing extension (demonstrated in Fig. 8) might include embedding analyte-sensitive images within the holographic medium – with perhaps a badge on an employee's uniform signaling a potential health risk. Among other attractive features, the technology behind commercial hologram design is well established for other applications, and accordingly holographic biosensor researchers have targeted markets in need of inexpensive, disposable, and mass-producible sensors.

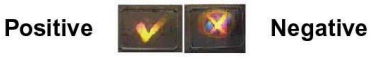

Fig. 8 Example of a holographic sensor with images observed in the presence (left) and absence (right) of a target species. (Courtesy of Christopher Lowe, University of Cambridge.)

Chemoresponsive diffraction gratings

Another promising interferometric sensing approach involves micropatterned diffraction gratings. There are two related approaches to this general chemical and biological sensing scheme. The first is based on gratings which have a very weak initial diffraction (small $d \cdot \Delta n$), not visible with the naked eye. When exposed to an analyte, $d \cdot \Delta n$ increases and the diffraction pattern 'appears'. Using this approach, sensors for bacteria[36,37] and proteins[38-43] have been demonstrated.

More recently, diffraction-based sensors have been investigated that display a diffraction pattern prior to analyte introduction[44-49]. In these systems, sensing is accomplished by monitoring, typically with inexpensive photodiodes, the changes in diffraction efficiency (fraction of light diffracted). Because molecular species are characterized by refractive indices greater than that of vacuum ($n = 1$), the diffraction efficiency of these chemosensors increases in response to volatile organic compounds (VOCs) as they fill voids within a porous sensing framework. For example, micropatterned polymeric gratings have been found to respond rapidly and reproducibly to a series of VOCs, with limits of detection below government-mandated exposure limits[47].

While the simplest grating-based sensors only make use of changes in the real component of the refractive index, others take advantage of changes in the imaginary component k of the complex refractive index, $\tilde{n} = n + ik$. The imaginary component of a material (or analyte) is closely related to its absorptivity. Enhanced analyte sensitivity can be obtained if target binding induces a color change, bringing the material's absorbance spectra more or less into registry with the probe laser beam. One demonstration of this makes use of a grating fabricated from 'vapochromic' material[48]. As the color of the material shifts as a result of analyte uptake, its absorbance becomes more or less resonant with the probe laser beam, eliciting dramatic resonance amplification and *de*amplification of sensor responses. Fig. 9 shows analyte uptake curves measured with probe lasers of different wavelengths, showing a 3500-fold amplification in sensor response when the probe wavelength is changed from nonresonant to resonant.

An initially unexpected, yet equally important, consequence of this effect is that resonance enhancement can be engendered selectively. Two analytes sorbed in similar amounts, yet inducing different perturbations to the grating material's absorbance, are easily distinguished via a multicolor

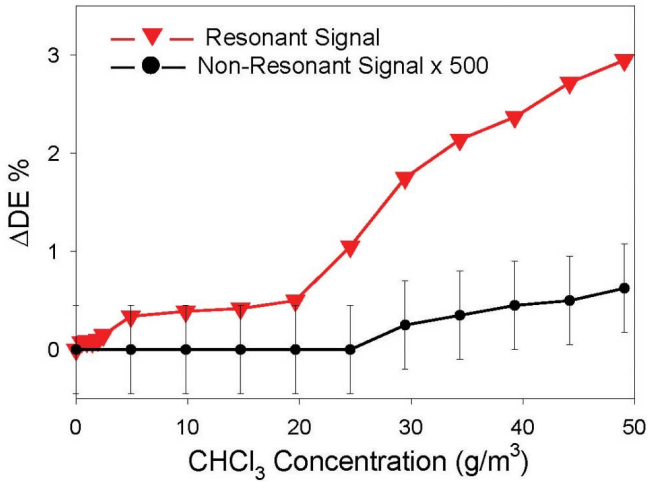

Fig. 9 Diffraction signal intensities (ΔDE% = changes in relative diffraction efficiency) for chloroform vapor uptake by a clathrate-forming charge-transfer salt that absorbs visible light: red – resonant probe (▾ 632.8 nm); black – nonresonant probe (• 834 nm). Note that the response at 834 nm has been multiplied by 500 to facilitate comparisons. The signals measured at 632.8 nm are about 3500 times larger than those measured at 834 nm. (Reprinted with permission from[48]. © 2002 American Chemical Society.)

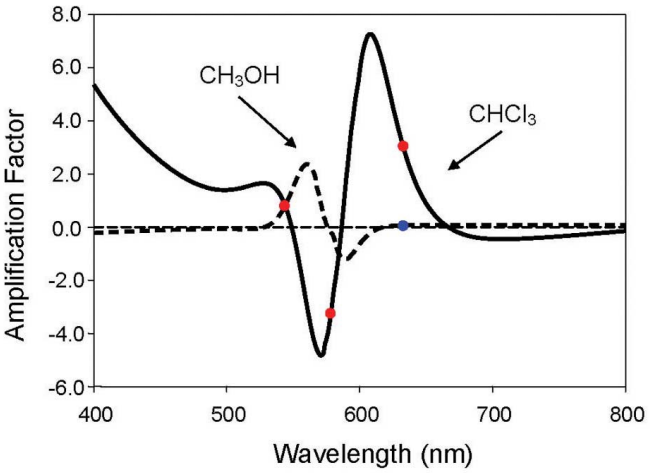

Fig. 10 Calculated wavelength-dependent diffraction responses of a resonantly illuminated diffraction grating upon exposure to chloroform (solid line) and methanol (dashed line). The points are experimental measurements. (Reprinted with permission from[48]. © 2002 American Chemical Society.)

diffraction-based assay. As illustrated in Fig. 10, the signal for chloroform at 633 nm is selectively amplified by over three orders of magnitude compared with methanol. Alternatively, measurements made at other wavelengths allow for the preferential detection of methanol. Notice that, here, analyte specificity is amplified at the readout stage, further enhancing differentiation beyond inherent material limits of target sorption and/or binding, as well as suggesting an approach towards 'nulling-out' responses from interfering species.

As an extension into biosensing, resonantly enhanced diffraction gratings have been constructed for the detection of oligonucleotides in real time[49]. Using nanoparticle-labeled DNA probes, single-stranded oligonucleotide targets are detected on binding to complementary-functionalized diffraction gratings. Analogous to the previously described vapochromic gratings, the optical properties of captured nanoparticles provide an optical signature in multiwavelength diffraction measurements. The analytical significance of this observation, combined with the corresponding theoretical understanding, points to the intriguing possibility of target multiplexing. This might be realized by encoding different target biomolecules with unique nanoparticle labels, each with a different shape, size, and/or composition, and thus possessing unique optical properties.

Conclusions

The work highlighted above, while not all-inclusive, is representative of the many exciting developments underway in the field of interferometric chemical and biological sensing. The technologies described are characterized by mechanical simplicity, reasonable cost, and potentially simple readout.

One clear attraction of interferometric sensors is that they could serve as 'universal' sensors. The basis for the potential universality is that all molecules contain polarizable electrons. Consequently, all have refractive indices greater than unity, and thus will alter the refractive index contrast of a device relative to vacuum (n = 1). Similarly, the anomalously low refractive index of water (n = 1.33) points to the feasibility of aqueous-phase detection of most water-borne analytes. Advances in the area of soft-materials micropatterning and microstructuring are facilitating the broad application of these technologies, at least at the proof-of-principle level. Another attractive feature of interferometric sensors is the potential for resonance amplification, resulting in enhanced sensitivity and selectivity. While demonstrated so far only for chemoresponsive diffraction gratings, there may be ways to adapt the idea to related sensor platforms. Besides being an active area of research in many academic laboratories, interferometric chemical and biological sensing has attracted the attention of several industrial ventures. Indeed, at least five companies are now driving interference-based sensing technologies towards commercialization. MT

REFERENCES

1. Xia, Y., and Whitesides, G. M., *Angew. Chem. Int. Ed.* (1998) **37** (5), 550
2. Stein, A., and Schroden, R. C., *Curr. Op. Solid State Mater. Sci.* (2001) **5** (6), 553
3. Velev, O. D., and Lenhoff, A. M., *Curr. Op. Colloid Interface Sci.* (2000) **5** (1-2), 56
4. Thompson, G. E., *Thin Solid Films* (1997) **297** (1-2), 192
5. Cullis, A. G., *et al., Appl. Phys.* (1997) **82** (3), 909
6. Lin, V. S., *et al., Science* (1997) **278**, 840
7. Janshoff, A., *et al., J. Am. Chem. Soc.* (1998) **120** (46), 12 108
8. Dancil, K. P. S., *et al., J. Am. Chem. Soc.* (1999) **121** (34), 7925
9. Gao, J., *et al., Appl. Phys. Lett.* (2000) **77** (6), 901
10. Létant, S., and Sailor, M. J., *Adv. Mater.* (2000) **12** (5), 355
11. Létant, S. E., *et al., Sens. Actuators B* (2000) **69** (1-2), 193-198
12. Sohn, H., *et al., J. Am. Chem. Soc.* (2000) **122** (22), 5399
13. Létant, S., and Sailor, M. J., *Adv. Mater.* (2001) **13**, 335
14. Cunin, F., *et al., Nat. Mater.* (2002) **1** (1), 39
15. Gao, J., *et al., Langmuir* (2002) **18** (6), 2229
16. Schmedake, T. A., *et al., Adv. Mater.* (2002) **14** (18), 1270
17. Rocchia, M. A., *et al., Phys. Status Solidi A* (2003) **19** (2), 365
18. Link, J. R., and Sailor, M. J., *Proc. Natl. Acad. Sci. USA* (2003) **100** (19), 10 607
19. Pan, S., and Rothberg, L. J., *Nano. Lett.* (2003) **3** (6), 811
20. Chan, S., *et al., J. Am. Chem. Soc.* (2001) **123** (47), 11 797
21. Holtz, J. H., and Asher, S. A., *Nature* (1997) **389**, 829
22. Holtz, J. H., *et al., Anal. Chem.* (1998) **70** (4), 780
23. Lee, K., and Asher, S. A., *J. Am. Chem. Soc.* (2000) **122** (39), 9534
24. Reese, C., *et al., Anal. Chem.* (2001) **73** (21), 5038
25. Asher, S., *et al., Anal. Bioanal. Chem.* (2002) **373** (7), 632
26. Alexeev, V. L., *et al., Anal. Chem.* (2003) **75** (10), 2316
27. Alexeev, V. L., *et al., J. Am Chem. Soc.* (2003) **125** (11), 3322
28. Asher, S. A., *et al., Anal. Chem.* (2003) **75** (7), 1676
29. Reese, C. E., and Asher, S. A., *Anal. Chem.* (2003) **75** (15), 3915
30. Sharma, A., *et al., J. Am. Chem. Soc.* (2004) **126** (9), 2971
31. Alexeev, V. L., *et al., Clin. Chem.* (2004) **50** (12), 2353
32. Carlson, R. J., and Asher, S. A., *Appl. Spectrosc.* (1984) **38** (3), 297
33. Millington, R. B., *et al., Anal. Chem.* (1995) **67** (23), 4229
34. Marshall, R. J., *et al., Anal. Chem.* (2003) **75** (17), 4423
35. Marshall, R. J., *et al., Anal. Chem.* (2004) **76** (5), 1518
36. St. John, P. M., *et al., Anal. Chem.* (1998) **70** (6), 1108
37. Morhard, F., *et al., Sens. Actuators B* (2000) **70** (1–3), 232
38. Goh, J. B., *et al., Anal. Bioanal. Chem.* (2002) **374** (1), 54
39. Goh, J. B., *et al., Anal. Bioanal. Chem.* (2003) **313** (2), 262
40. Tsay, Y. G., *et al., Clin. Chem.* (1991) **37** (9), 1502
41. Cunningham, B., *et al., Sens. Actuators B* (2002) **81** (2-3), 316
42. Lin, B., *et al., Biosens. Bioelectron.* (2002) **17** (9), 827
43. Cunningham, B., *et al., Sens. Actuators B* (2002) **87** (2), 365
44. Bailey, R. C., *et al.*, In *Chemical and Biological Sensors and Analytical Methods II*, Butler, M., *et al.*, (eds.), The Electrochemical Society Proceedings, Pennington, NJ (2001), 511
45. Dang, X., *et al., Langmuir* (2001) **17** (11), 3109
46. Mines, G. A., *et al., Angew. Chem. Int. Ed.* (2002) **41** (1), 154
47. Bailey, R. C., and Hupp, J. T., *Anal. Chem.* (2003) **75** (10), 2392
48. Bailey, R. C., and Hupp, J. T., *J. Am. Chem. Soc.* (2002) **124** (23), 6767
49. Bailey, R. C., *et al., J. Am. Chem. Soc.* (2003) **125** (44), 13541